

The reference on the paper:

Nemergut M, Škrabana R, Berta M, Plückthun A, Sedlák E. Purification of MBP fusion proteins using engineered DARPin affinity matrix. *Int J Biol Macromol.* 2021 Sep 30;187:105-112. doi: 10.1016/j.ijbiomac.2021.07.117.

## **Efficient purification of MBP fusion proteins on DARPin affinity matrix**

Michal Nemergut<sup>a,b</sup>, Rostislav Škrabana<sup>c</sup>, Andreas Plückthun<sup>d</sup>, and Erik Sedlák<sup>a,\*</sup>

<sup>a</sup>Center for Interdisciplinary Biosciences, Technology and Innovation Park of P.J. Šafárik University, Jesenná 5, 041 54 Košice, Slovakia

<sup>b</sup>Department of Biophysics, Faculty of Science, P.J. Šafárik University, Jesenná 5, 041 54 Košice, Slovakia

<sup>c</sup>Institute of Neuroimmunology, Slovak Academy of Sciences, Dúbravská cesta 9, 845 10 Bratislava, Slovakia

<sup>d</sup>Department of Biochemistry, University of Zurich, Winterthurerstrasse 190, CH-8057 Zurich, Switzerland

To whom correspondence should be addressed: Center for Interdisciplinary Biosciences, Technology and Innovation Park of P.J. Šafárik University, Jesenná 5, 041 54 Košice, Slovakia; Email: [erik.sedlak@upjs.sk](mailto:erik.sedlak@upjs.sk)

## **Abstract**

Maltose binding protein (MBP) has a long history as an expression tag for the production of recombinant fusion proteins. The ability of MBP to increase the solubility of fusion proteins makes it a preferred option for the expression of recombinant proteins that are unable to fold properly or that tend to form aggregates. A critical step for obtaining a sufficient amount of the MBP fusion protein is the purification. Commercially available affinity chromatography for the purification of MBP fusion proteins using amylose matrix has two main issues: (i) low (micromolar) affinity and (ii) limited number of uses due to the cleavage of polysaccharide matrix by the amylases present in the crude cell extract. To avoid this problem, we developed an affinity chromatography based on the protein-protein interaction. We use an evolved Designed Ankyrin Repeat Protein off7 (DARPin off7), which interacts with MBP with almost 1000 times higher affinity than amylose. The functionality of such affinity chromatography was tested with the purification of MBP-tagged green fluorescent protein (GFP) and flavodoxin (FLD). The optimized affinity chromatography based on the MBP-DARPin off7 interaction enables the purification of the fusion proteins in a single-step procedure. This affinity column - easy to construct, resistant to amylase and reproducible for numerous purification cycles - provides an alternative approach to commercially available affinity chromatographies for purification of proteins containing the MBP tag.

## **Abbreviations**

CD - circular dichroism; CV - column volume; DSC - differential scanning calorimetry; IMAC - immobilized metal-ion affinity chromatography; IPTG - isopropyl- $\beta$ -D-thiogalactopyranoside; ITC - isothermal titration calorimetry; GFP - green fluorescent protein; FLD - flavodoxin; MBP - maltose binding protein; POI - protein of interest; SPR - surface plasmon resonance;

## 1. Introduction

Production of recombinant proteins in bacterial systems is often accompanied by accumulation of overexpressed proteins in the form of insoluble and biologically inactive aggregates [1]. One way how to address this issue is the expression of the protein of interest (POI) conjugated with a tag or domain that can enhance its solubility and even promote its proper folding. The most popular solubility tags are the maltose binding protein (MBP) [2,3], glutathione S-transferase [4], and thioredoxin [5]. Although the use of each tag has its advantages and disadvantages [6], it was shown that MBP possesses chaperone-like properties and is a better solubilizing agent than the GST or TRX [7–10]. Moreover, the natural periplasmic localization of MBP provides a suitable expression strategy for toxic proteins [11], antibody fragments [12–15] or membrane proteins [16,17]. All these positive effects of MBP on its fusion partners, the possibility of MBP to enhance the formation of crystal contacts and the fact that the MBP structure is known and may be used for solving the phase problem by molecular replacement make MBP the most successful crystallization chaperone [18,19]. The number of crystal structures of polypeptides fused to MBP has grown dramatically during the past decade, which resulted in more than one hundred solved structures available in the Protein Data Bank [20].

On the other hand, the major disadvantage of using MBP as an expression tag is the tedious purification of the MBP conjugates. Native MBP can be isolated from *E. coli* by its binding to amylose [21]. *New England Biolabs* developed vectors with multiple cloning sites for expression and purification of cytosolic as well as periplasmic MBP fusion proteins [2,3]. Later, in order to allow alternative purification possibilities, Nallamsetty et al. [22,23] designed constructs containing combinations of His-tag and MBP-tag. Despite the improvements made in this field, the weak affinity of MBP to amylose still remains the main obstacle of this purification strategy. A further limitation of amylose affinity chromatography is caused by the enzyme amylase and the disaccharide maltose, which are both present in the cell lysate. While the amylose matrix degradation by amylases causes a decrease in binding capacity of the column and reduces the number of column regeneration cycles, the presence of maltose in the cell lysate causes elution of the MBP fusion proteins from the amylose matrix [24,25].

In an effort to overcome the limitations of the amylose chromatography, we developed a new affinity chromatography for purification of MBP, based on protein-protein interaction. Designed Ankyrin Repeat Protein off7 (DARPin off7) evolved to bind to MBP with high affinity and specificity was used as an immobilized ligand responsible for MBP binding [26]. The affinity column matrix enables: (i) the purification of MBP fusion proteins in a single-step

procedure and (ii) numerous repetitive column regenerations without affecting the binding properties of the DARPin off7. The presented alternative affinity chromatography for the purification of MBP fusion proteins exhibits better yield and ability of regeneration than currently available polysaccharide affinity matrices.

## 2. Material and methods

### 2.1. MBP fusion proteins cloning

MBP fusion proteins were expressed using a modified pQE-30 vector containing the open reading frame of MBP, which was extended with a human rhinovirus 3C protease cleavage motif (LEVLFQGP). The open reading frames encoding GFP and FLD were amplified by PCR with introducing *Bam*HI and *Hind*III sites at the N- and C- terminal sequences, respectively. The resulting PCR amplicons were digested with *Bam*HI and *Hind*III (New England BioLabs, Ipswich, Massachusetts, USA), and then ligated with the *Bam*HI/*Hind*III vector backbone of pQE-30 to create the final expression vector. The nucleotide sequences were verified experimentally.

### 2.2. Site-directed mutagenesis

Defined point mutations (K17R, K144R and K147R) were introduced in the binding interface of DARPin off7 using the QuikChange site-directed mutagenesis kit (Agilent Technologies, Santa Clara, California, USA). The synthesized oligonucleotide primers (Microsynth AG, Switzerland) containing the desired mutations (Table 1) were used in consecutive PCR reactions to generate different DARPin off7 mutants. After temperature cycling, the PCR products were treated with *Dpn*I and the nicked plasmids containing the desired mutations were then transformed into home-made XL1-Blue competent cells.

**Table 1.** List of primers used for site-directed mutagenesis.

K17R mutation	
forward	5'-CCGACCTGGGTAGGAGACTGCTGGAAGCTGCTCGTGCTGG-3'
reverse	5'-CCAGCACGAGCAGCTTCCAGCAGTCTCCTACCCAGGTCGG-3'
K114R a K147R double mutations	
forward	5'-CGCTCAGGACAGATTCGGTAGGACCGCTTTCGACATCTCCATC G-3'
reverse	5'-CGATGGAGATGTCGAAAGCGGTCCTACCGAATCTGTC CTGAGC G-3'

### 2.3. Protein expression

All studied proteins were expressed in the *E. coli* strains XL1-Blue or BL21 (3C protease). 2xYT medium containing 100 µg/ml ampicillin (35 µg/ml kanamycin in the case of

the 3C protease) and 0.4% glucose was inoculated to  $OD_{600} \sim 0.1$  with an overnight pre-culture harbouring a corresponding expression plasmid. Protein expression at  $37^{\circ}\text{C}$  was induced with 1 mM IPTG upon reaching  $OD_{600} \sim 0.6$  and continued for the next 4 hours. After incubation, the cells were harvested by centrifugation (15 min, 5000 g,  $4^{\circ}\text{C}$ ) and frozen in liquid nitrogen till they were further proceed.

#### 2.4. Purification of DARPin, MBP and 3C protease

All the following steps were carried out on the ice and with cooled ( $4^{\circ}\text{C}$ ) buffers. The cell pellet was resuspended in TBS lysis buffer pH 8.0 (4 ml/g) containing 50 mM Tris-HCl, 400 mM NaCl and lysozyme (1.5 mg/ml). Subsequently, the resuspended cells were incubated for 30 minutes with 1 mM EDTA and 1  $\mu\text{l}$  of protease inhibitors (5  $\mu\text{g}/\text{ml}$  of leupeptin and 1  $\mu\text{g}/\text{ml}$  of pepstatin) per 1 ml of the resuspended pellet. Small amounts (on a spatula tip) of DNase I and 6 mM  $\text{MgCl}_2$  were added and the suspension was incubated for another 30 minutes. The cells were disrupted using sonification (Branson sonifier 450, Fisher Scientific) and cell debris was removed by centrifugation (35 min, 17,000 g,  $4^{\circ}\text{C}$ ). The filtrated supernatant was applied to a pre-equilibrated IMAC column (Ni-NTA Superflow resin, Qiagen) and washed with 10 column volumes (CV) of TBS washing buffer pH 8.0 (50 mM Tris-HCl, 400 mM NaCl pH, 20 mM imidazole and 10% glycerol), 10 CV of TBS low-salt buffer pH 8.0 (50 mM Tris-HCl, 20 mM NaCl, 20 mM imidazole and 10% glycerol), 10 CV of TBS high-salt buffer pH 8.0 (50 mM Tris-HCl, 1 M NaCl pH, 20 mM imidazole and 10% glycerol) and again 10 CV of TBS washing buffer. Finally, the proteins were eluted with TBS elution buffer pH 7.4 (50 mM Tris-HCl, 400 mM NaCl pH, 250 mM imidazole and 10% glycerol), frozen in liquid nitrogen and stored at  $-80^{\circ}\text{C}$ .

#### 2.5. Preparation of DARPin off7 affinity column

NHS-activated Sepharose 4 Fast Flow (GE Healthcare, 2 ml of slurry) was poured into empty PD-10 desalting column and washed immediately with 10 ml of ice-cold 1 mM HCl. Subsequently, 1 ml of 20 mg/ml of the purified DARPin off7 in coupling buffer (0.2 M  $\text{NaHCO}_3$ , 0.5 M NaCl, pH 8.3) was added and incubated for 3 hours at room temperature. After the coupling reaction was completed, the column was drained and a flow-through was further tested with a Biuret assay in order to determine the coupling efficiency. To block unreacted NHS-groups, the column was incubated overnight with 0.1 M Tris-HCl, pH 8.5 at  $4^{\circ}\text{C}$ . Finally, the column was washed 3-times with 0.1 M  $\text{CH}_3\text{COONa}$ , 0.5 M NaCl pH 4.5 and 0.1 M Tris-HCl pH 8.5 in an alternative manner. To prevent microbial contamination, the column was stored in 20% ethanol.

## 2.6. Circular dichroism (CD)

The experiments were performed using a Jasco J-810 spectropolarimeter (Tokyo, Japan). Ellipticity in the far-UV region was measured at room temperature with a 1 mm pathlength quartz cuvette. The experiments were performed in 50 mM glycine (pH 3.5 and pH 2.7) or in 50 mM phosphate buffer (pH 7.0) with the protein concentrations of 10  $\mu$ M.

## 2.7. Isothermal titration calorimetry (ITC)

ITC experiments were performed using a MicroCal iT200 system from Malvern. In the experiments related to the study of the interaction recovery, the proteins were dialyzed against a buffer containing 50 mM glycine pH 3.5 and then against 50 mM phosphate buffer pH 7.0. All other experiments were performed with PBS pH 7.4. The protein solutions were degassed prior to titration. In all cases, DARPin off7 from a 500  $\mu$ M stock solution was titrated into a 50  $\mu$ M solution of MBP. The calorimetry cells were thermostated at 23 °C and each injection was separated by 180 s. The baseline, calculated as an average of the normalized heat per injection value of the extra injections at the end of the experiment, was subtracted and data were fit with the Origin software provided with the instrument.

## 2.8. Differential scanning calorimetry (DSC)

DSC measurements were performed using a VP-Capillary DSC system (Microcal Inc., acquired by Malvern Instruments Ltd.). The proteins were dialyzed against the corresponding buffers in the same manner as in the ITC experiments. The protein concentrations were adjusted to 23  $\mu$ M and all samples were degassed prior to measurement. The samples were heated from 25°C to 90°C with a scan rate of 0.5 K/min. Thermograms were corrected by subtraction of the so-called chemical baseline, i.e., the sigmoidal curve connecting the signal of excess heat capacity of the native and denatured states, and normalized to the molar concentration of the protein.

## 2.9. Surface plasmon resonance measurements (SRP)

SPR experiments were performed using BIAcore 3000 (GE Healthcare). DARPin off7 was modified by substoichiometric coupling of an amine-reactive biotin reagent to achieve preferential immobilization via His-tag on an SA chip (GE Healthcare). The measurement was carried out at 25°C with degassed buffers containing 0.005% Tween 20. The reversibility of the interaction between immobilized DARPin off7 and 50 nM MBP was measured in 50 mM phosphate pH 7.0, followed by regenerating the immobilized DARPin with 100 mM glycine pH 3.5, and then reapplying fresh MBP in 50 mM phosphate pH 7.0 containing 50 nM MBP.

### 3. Results

The existence of a specific interaction with the high affinity between DARPin off7 and MBP at neutral pH had been demonstrated previously [26]. However, for repetitive use of any affinity chromatography matrix, it is inevitable to find conditions in which the specific interaction between protein and ligand is perturbed in a reversible manner. Such perturbation, in general, can be achieved, for example, by chemical denaturants, such as urea or guanidium chloride, or extreme pH. Due to the high resistance and conformational stability of DARPins against chemical denaturants [27], we tested the effect of an acidic pH on stability and reversibility of conformational states of both proteins.

#### 3.1. Conformation and binding properties of DARPin off7 and MBP at different pH

Conformational properties of DARPin off7 and MBP under different pH conditions were investigated by CD and DSC. While an ellipticity in the far-UV region reflects the protein secondary structure, the protein thermal stability determined by DSC is related to the changes of the tertiary structure of the protein. CD spectra and DSC thermograms were collected within a broad pH region, from pH 2.7 to pH 10.0 (Fig. S1 and S2). The largest structural changes were observed at acidic pHs (Fig. 1).

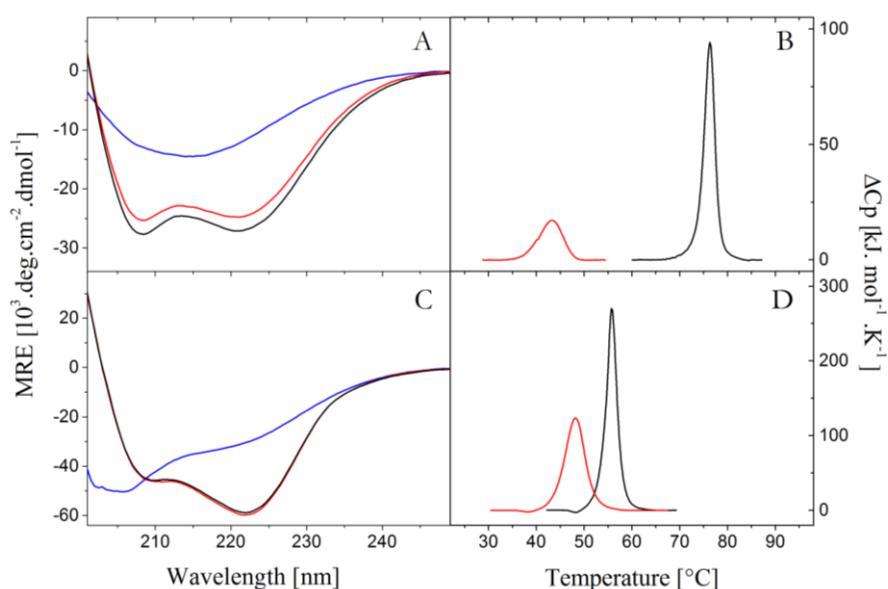


**Fig. 1.** CD spectra in the far-UV spectral region and DSC thermograms of DARPin off7 (A, B) and MBP (C, D), respectively. pH 7.0 (**black**), pH 3.5 (**red**) and pH 2.7 (**blue**).

The most significant ellipticity changes in both proteins occur below pH 3.0 and reflect a large decrease of the protein secondary structures. On the other hand, a shift of the DARPin

off7 transition temperature to lower temperatures at pH 3.5 (more than 30 °C) clearly indicates significant perturbation of its tertiary structure already at this pH value. A smaller relative decrease in transition temperature in the case of MBP (about 7.5 °C) when going from pH 7.0 to 3.5 also suggests a destabilization of MBP conformation at pH 3.5, as MBP had a lower transition temperature already at neutral pH.

The exposure of DARPin off7 and MBP conjugate to acidic pH in the column regeneration process may be accompanied by irreversible changes in the protein structures. Therefore, it is necessary to determine whether observed structural changes in the proteins are reversible and the interaction between them is fully recovered. The structure recovery of both proteins, as well as their complex, was determined after a 4-hour incubation at pH 3.5 with a subsequent transition back to pH 7.0 (Fig. 2). DSC transition curves were virtually identical, demonstrating that the structural changes under acidic conditions are entirely reversible.

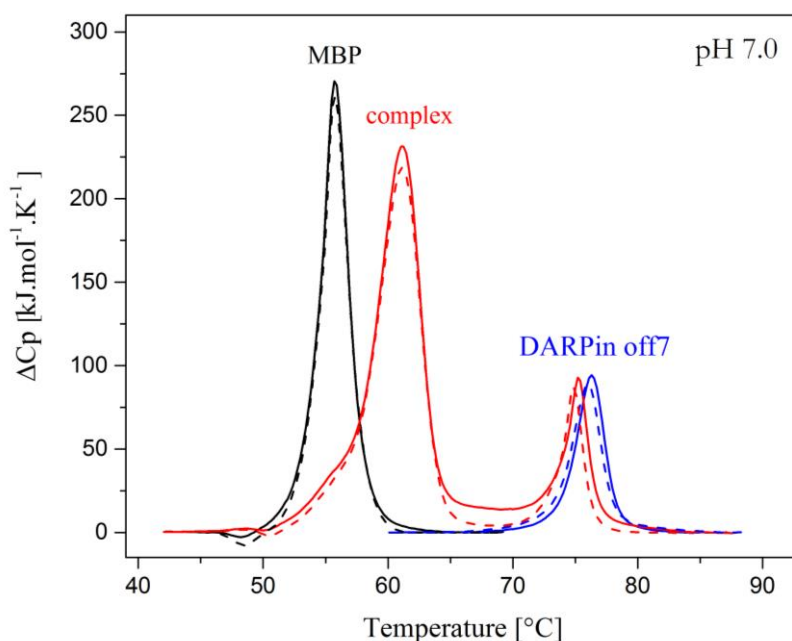


**Fig. 2.** DSC thermograms showing the thermal stability of MBP (**black**), DARPin off7 (**blue**) and DARPin off7/MBP complex (**red**). Solid lines represent the original thermal transitions of the proteins at pH 7.0. Dashed lines represent thermal transitions of the proteins after exposure to and acidic environment of pH 3.5 back for 4 hours, after brought back to a neutral environment of pH 7.0.

The DARPin off7/MBP complex formation can be followed also by DSC. In fact, the binding of DARPin off7 to MBP leads to a shift of transition temperature of the MBP complex at pH 7.0 by 5.5 °C in comparison to free MBP. This shift indicates a strong interaction between these proteins. Using Brandts' theoretical model [28], which allows determining the binding



affinity of two interacting proteins from DSC measurements, we were able to determine the dissociation constant of the DARPin off7-MBP interaction in the low nanomolar range,  $K_D \sim 1.5$  nM, consistent with the previously measured affinity by SPR [26].

The influence of acidic pH on the interaction between the DARPin off7 and MBP was also analyzed by SPR (Fig. 3A) and ITC (Fig. 3B). The obtained results from both SPR and ITC techniques confirmed a strong interaction at pH 7.0, reflected by  $K_D = 7.7 \pm 1.3$  nM and  $47 \pm 3$  nM, respectively. No binding at pH 3.5 was detected by these methods. Both techniques showed almost identical binding curves obtained after neutral-acidic-neutral exposure as before pH transition. These results support the ability of the proteins to refold properly back into their native states after their exposure to the acidic pH=3.5.

MBP-tagged recombinant proteins are commonly eluted from an amylose column by

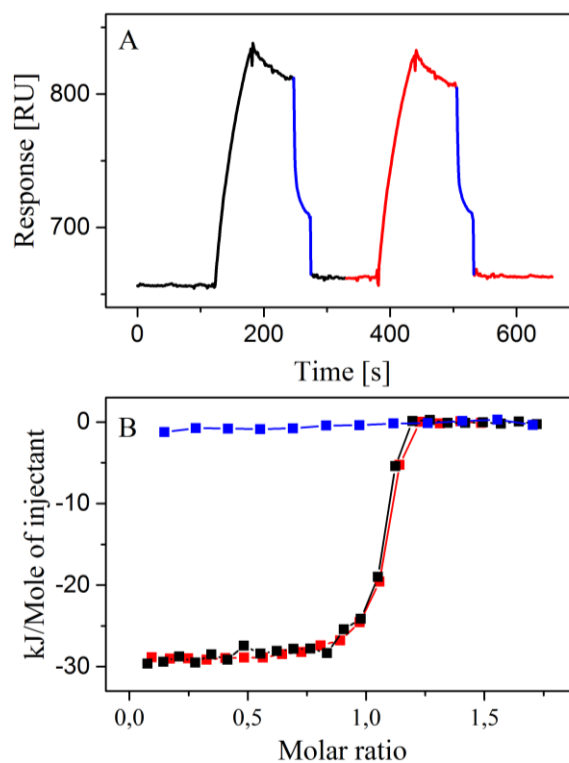


**Fig. 3.** pH dependence of the interaction between DARPin off7 and 50 nM MBP. (A) SPR experiment: first binding of MBP to immobilized off7 at pH 7.0 and dissociation (**black**), regeneration by dissociation of bound MBP at pH 3.5 (**blue**), and the second run at pH 7.0 (**red**). (B) ITC experiment: binding events at pH 7.0 (**black**), at pH 3.5 (**blue**) and at pH 7.0 after shifting back from acidic to neutral condition (**red**).

10 mM maltose solution. Therefore, the influence of maltose on the DARPin off7 and MBP complex formation was examined. The formation of the DARPin off7/MBP complex was examined by ITC in the presence of two different maltose concentrations, 250 mM and 400

mM (Fig. S3). The similarity of the binding curves strongly indicates that maltose does not affect the affinity as well as other thermodynamic parameters of the interaction between DARPin off7 and MBP (Table S1). This is not an unexpected result because maltose and DARPin off7 binding sites on the MBP are distant from each other. However, it was important to find out whether maltose may affect the DARPin off7-MBP interaction due to the relatively large conformational change of MBP upon maltose binding [29,30].

### 3.2. Isolation of MBP fusion proteins

In order to test the DARPin off7 affinity column, we constructed two different MBP fusion proteins. Green fluorescent protein (GFP, MW: 27.3 kDa) and flavodoxin (FLD, MW: 16.3 kDa) were fused to MBP (MW: 43.1 kDa) through the linker containing a 3C protease cleavage site and expressed in *E. coli*. The MBP fusion protein bound to the DARPin off7 matrix was either eluted with 100 mM glycine buffer of pH 3.5 or it was incubated for 2 hours at room temperature with 3C protease and then the flow-through was collected. The application of 100 mM glycine of pH 3.5 led to elution of the whole MBP conjugate (Fig. 4A) while the 3C protease cleavage directly eluted the purified POI (Fig. 4B). The fact that 3C protease was added directly onto the column was responsible that this enzyme was collected together with

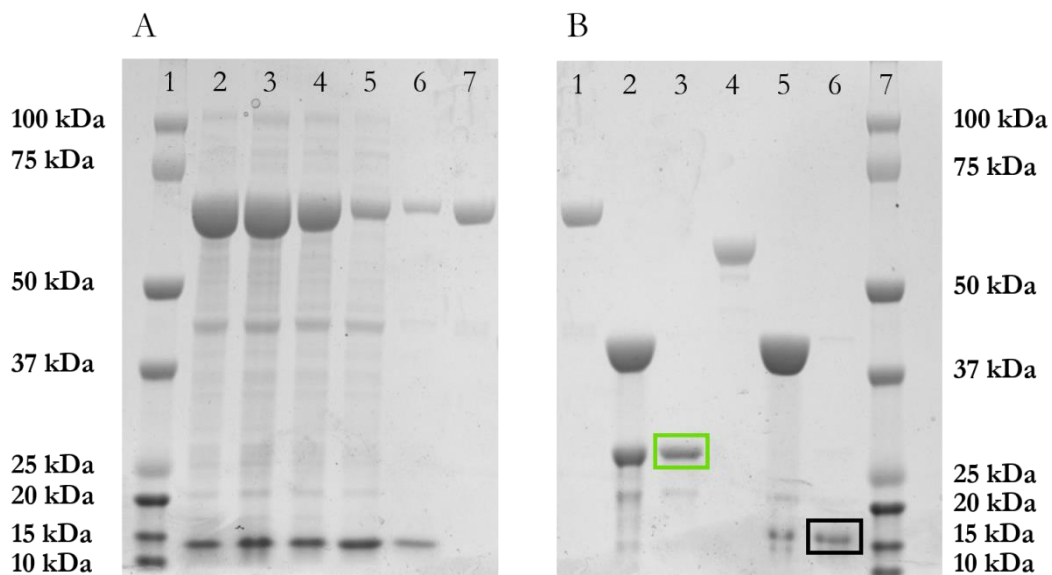


**Fig. 4.** Isolation of MBP fusion proteins by DARPin off7 affinity column. (A) Whole process of MBP-GFP isolation: 1 – molecular weight standard, 2 – cell lysate upon loading a large excess of the fusion protein, 3 – flow-through, 4 – 1<sup>st</sup> CV of washing buffer, 5 – 2<sup>nd</sup> CV of washing buffer, 6 – 3<sup>rd</sup> CV of washing buffer, 7 – MBP-GFP elution by 100 mM glycine of pH 3.5; (B) Cleavage of MBP fusion proteins: 1 – MBP-GFP, 2 – MBP-GFP cleavage by 3C protease, 3 – purified GFP (green frame), 4 – MBP-FLD, 5 – MBP-FLD cleavage by 3C protease, 6 – purified FLD (black frame), 7 – molecular weight standard.

desired recombinant protein (weak band at 22 kDa in Fig. 4B line 3). A 3C protease amount of a total of 2% w/w of target protein was sufficient to efficiently cleave all MBP conjugates.

To remove the 3C protease, the protein mixture was further purified by reverse IMAC and, finally, polished by gel filtration chromatography, yielding a pure and homogeneous preparation (Fig. 5).

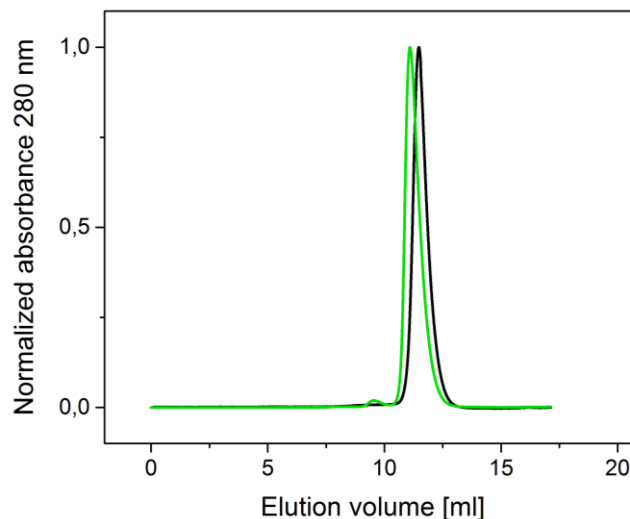


**Fig. 5.** Size exclusion chromatography of the purified FLD (**black**) and GFP (**green**) detected by Sepharose Increase 75 in PBS. The chromatograms of GFP and FLD consist of single peaks demonstrating a high purity and homogeneity of the proteins.

### 3.3. Binding capacity optimization

The DARPin off7 molecules are covalently conjugated to the column matrix through the amino groups of lysine residues, even though a coupling through the N-terminal amine may also occur. Since DARPin off7 contains 8 lysine residues on both sides of the molecule (Fig. 6) it may bind to the sepharose resin in a random manner. An attachment of DARPin off7 through Lys17, Lys144 or Lys 147 would sterically inhibit the interaction of DARPin off7 with MBP (Fig. 6). In an effort to improve the binding capacity of the DARPin off7 column by preventing the reaction of these lysine residues with the resin, they were replaced by mutation to arginine. Lysine 121 is a part of the selected randomized residues, therefore it was not replaced. DARPin off7 mutants containing various combinations of K17R, K144R or K147R were expressed and purified through IMAC (Fig. S4): (i) M1 containing the single mutation K17R, (ii) M2 containing two mutations, K144R and K147R, and (iii) M3 containing all three mutations, K17R, K144R and K147R. Expression of all DARPin off7 variants resulted in more than 100 mg per liter of a medium of the purified proteins.

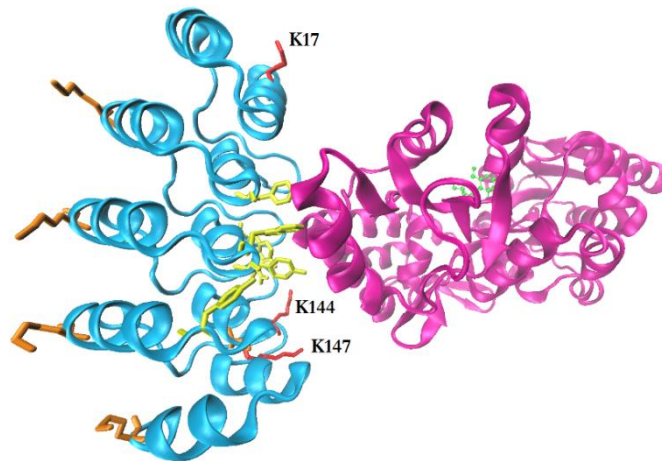


**Fig. 6.** Structure of DARPin off7/MBP complex with highlighted Lys residues and a maltose molecule bound to MBP (superposition of the crystal structures PDB ID: 1SVX and 1ANF). DARPin off7 is shown in light blue, MBP in purple, maltose in green, Lys residues able to covalently bind the resin in sticks, Lys residues (K17, K144, and K147) that were replaced with Arg are shown in red. The DARPin off7 residues responsible for the interaction with MBP are shown in yellow.

The SDS-PAGE of the purified variants of DARPin off7 did not show any contaminants, but size exclusion chromatograms of all the variants consist of one major peak constituting the monomer and one smaller peak (Fig. S5). The position of the smaller peak strongly suggests the presence of a dimeric form in the DARPin off7 population which increases with an increasing number of mutations.

#### 3.4. Binding properties of DARPin off7 variants.

The binding properties of the DARPin off7 variants were determined by ITC (Fig. 7). The analysis of the binding curves revealed the effect of the mutations on the thermodynamic

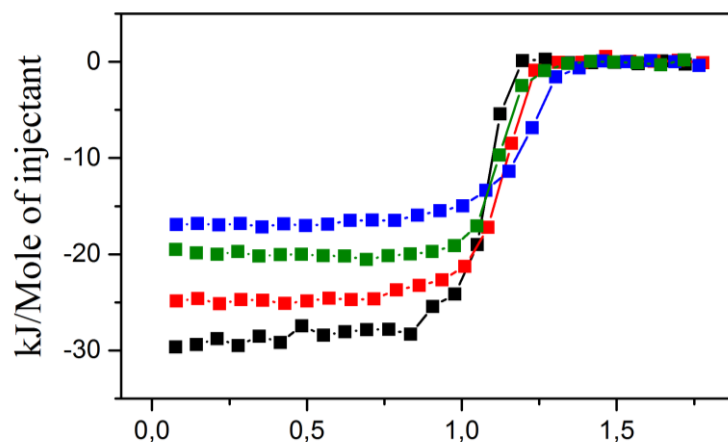


**Fig. 7.** ITC experiments showing the interaction of DARPin off7 variants with MBP. The DARPin off7 variants: WT (black), M1 (red), M2 (blue), and M3 (green).

parameters of the protein-protein interaction (Table S2). Although the mutated residues on DARPin off7 are distant from the site that participates in the interaction with MBP, the changes in the affinity of the variants were apparent. The weakest binding affinity was observed for the M2 variant,  $K_D = 114 \pm 2$  nM. The variants M1 and M3 are characterized by comparable affinity to MBP as the wild type with  $K_D = 65 \pm 4$  nM and  $K_D = 41 \pm 2$  nM, respectively. We note that the value of  $K_D$  for MBP wild type obtained by ITC are higher than previously obtained data by surface plasmon resonance [26] likely due to limitations of ITC at such high affinity interactions. However, we believe that the determined  $K_D$  values for the MBP wild type and its mutants obtained by ITC correctly express relative affinities of the MBP-off7 interaction.

### 3.5. The binding capacity of the columns containing the DARPin off7 wt and its variants

In order to determine a binding capacity of the DARPin off7 variants, 20 mg of the DARPin off7 variants were separately immobilized to 1 ml of sepharose resin. Prepared columns were used for purification of MBP-FLD and MBP-GFP conjugates (Fig. 8).

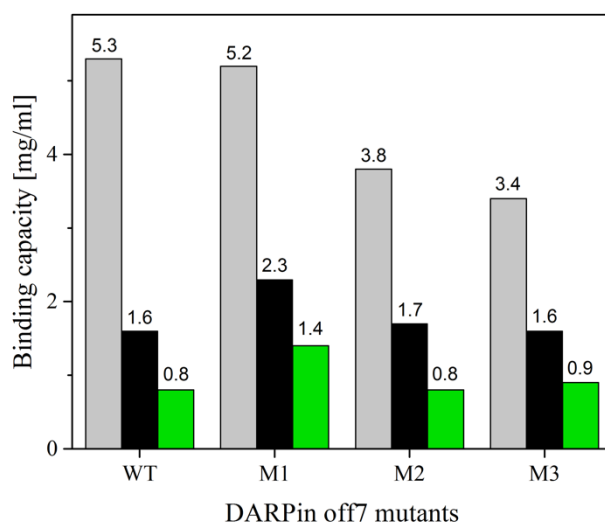


**Fig. 8:** Comparison of the binding capacity of the columns containing different DARPin off7 variants. The amount of the purified proteins per ml of the column matrix is listed at the corresponding columns. The purified proteins were: MBP (gray), MBP-FLD (black), and MBP-GFP (green).

A comparison of the binding capacity of the DARPin off7 variants revealed that the binding capacity for MBP itself is larger than for MBP fusion proteins. This phenomenon is commonly observed and it is probably caused by a blocking of additional MBP binding site by the size of the fusion protein [24]. Moreover, the binding capacity of the column does not

correlate with the number of mutations. In the case of the purification of MBP itself, the column binding capacity decreases with the increasing number of mutations. On the other hand, in the case of MBP-GFP and MBP-FLD purification, the highest binding capacity is observed for the matrix containing mutant M1; mutants M2 and M3 have a similar capacity as the wild type.

## 4. Discussion

### 4.1. Comparison of DARPin off7 with amylose resins

Due to its excellent solubilizing properties, MBP is often used for the purification of recombinant proteins that are not able to fold properly or that have to be expressed in the oxidizing environment of the periplasm. Purification of proteins fused to MBP can be made to result in purified POI alone or the whole MBP-POI conjugate (Fig. 9). The pure POI is usually utilized in the subsequent conformational and/or functional studies. The conjugate MBP-POI can be used as an alternative approach in protein crystallography when a standard way does not work [20], or in further immobilization of the POI if a solid phase is needed for particular assays.

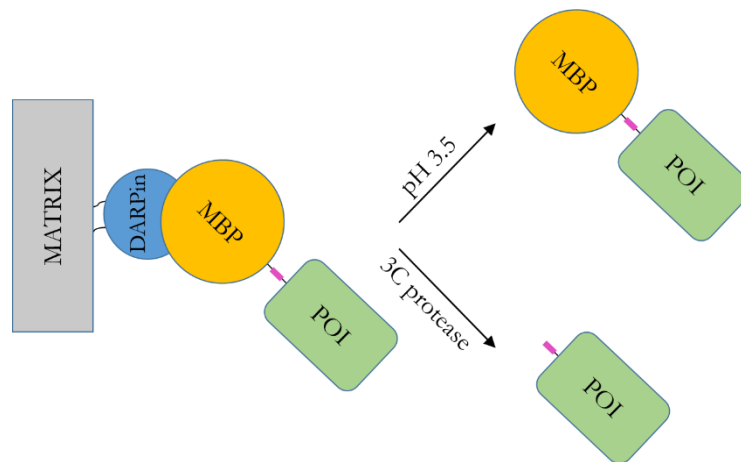


**Fig. 9.** Schematic representation of MBP fusion protein purification by DARPin off7 affinity column.

MBP is considered as one of the best solubility tags, but on the other hand as a relatively poor affinity tag. Several attempts were made to improve the purification strategy of MBP fusion proteins. Marvin and Hellenga [31] increased the binding affinity of MBP to maltose by specific point mutations. Nallamsety et al. [22] used an additional His-tag to avoid purification over amylose resin. While these attempts were aimed at modifying the MBP tag properties, we focused on an improvement of the matrix by using DARPin off7 as an affinity ligand. The

DARPin off7 was evolved by using ribosome display [32] to bind MBP with very high, low nanomolar affinity and high specificity [26]. For dissociating the DARPin off7/MBP complex, one may use chemical denaturants or extreme pHs. In our hands, the most efficient method was acidic pH  $\leq 3.5$ . From a practical point of view, the ability of DARPin off7 to recover its native structure and binding properties after exposure to acidic pH is crucial for the column regeneration, and it is useful that MBP does this, too. We found out that the DARPin off7 resin can be used consecutively at least 10 times without significantly decreased binding capacity towards MBP, in the contrast to amylose resin, where the number of runs is typically limited to 3-5 times, due to enzymatic degradation of amylose [24].

Buffers with pH  $\leq 3.5$  are the most commonly used elution buffer for affinity purification based on protein-protein interaction [33]. However, such pH may have a deleterious effect on some less stable proteins. One may avoid the elution of POI by acidic pH by performing on-column enzymatic cleavage by 3C protease. Application of a high-performance protease such as 3C leads to only small contamination of the used enzyme in eluted fraction, nonetheless, further purification steps will become necessary. In our case, 2% (w/w) 3C protease was sufficient to separate all POI from bound MBP. In contrast, amylose affinity purification does not allow efficient elution of fusion proteins directly on the column, and therefore, a standard purification protocol consists of several steps [25]. Firstly, bound MBP-POI is eluted with maltose, then it is enzymatically cleaved and finally, the POI is separated from MBP in the second amylose affinity purification. In addition, before repeated binding of MBP to amylose matrix can be carried out, proper removal of maltose from cleaved MBP is indispensable [24].

In order to improve this time-consuming purification, Nallamesty et al. [9,22] designed a His<sub>6</sub>-MBP tag that allows purification of MBP fusion proteins through IMAC. Although it has been shown that a His-tag at N-terminus of MBP does not influence MBP's solubilizing properties, its low specificity causes the presence of contaminants in the purified POI. Therefore, most of the His<sub>tag</sub>-MBP fusion protein purification methods include a combination of IMAC and amylose media or other purification procedures [6,15,20].

It is well known that MBP undergoes a relatively large conformational change upon maltose binding [29,30]. This structural reorganization can lead to complications. For example, Cherry et al. [34] obtained a different crystal structure of the SUFU-MBP conjugate in the presence and in the absence of maltose. In another case, Matsumoto and his colleagues [35] were able to obtain protein crystals only in the absence of maltose. Therefore, our single-step

purification not only saves time but also avoids obstacles related to maltose elution in the purification of the whole MBP-POI conjugates for crystallographic purpose.

#### 4.2. Purification of MBP fusion proteins by DARPin off7 column

An affinity almost a thousand times higher affinity of DARPin off7 to MBP in comparison to the affinity of MBP – sugar complexes [36] allows for more efficient MBP-POI purification. While a commercially available amylose resin has a binding capacity of 3 mg/ml of MBP, 1 ml of matrix containing 20 mg DARPin off7 can bind about 5 mg of MBP. In order to improve the binding capacity of our column, we introduced specific mutations at Lys residues to optimize the spatial orientation of the DARPin off7 with respect to the matrix (Fig. 10).

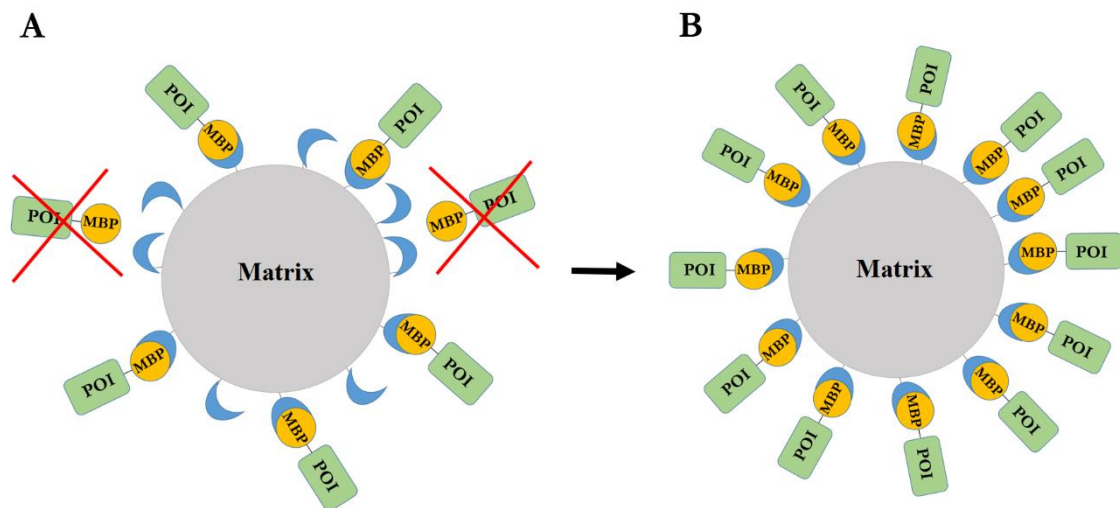


**Fig. 10.** Schematic representation of DARPin off7 spatial optimization.

## 5. Conclusions

The presented chromatographic purification method based on the interaction between MBP and DARPin off7 provides a fast and effective alternative approach for the purification of MBP fusion proteins. DARPin off7 expression and purification through IMAC, along with the column preparation, is a simple and inexpensive procedure which can be easily accomplished within three days and at large scales. Moreover, due to high stability of DARPin off7, the prepared matrix can be stored in a refrigerator for several weeks (and probably much longer) without affecting its binding properties.

## CRediT authorship contribution statement



**Michal Nemergut:** Investigation, Formal analysis, Writing – Original Draft **Rostislav Škrabana:** Investigation, Formal analysis **Andreas Plückthun:** Conceptualization, Writing – Review & Editing **Erik Sedlák:** Funding acquisition, Formal analysis, Writing – Review & Editing.

#### **Declaration of competing interest**

None.

#### **Acknowledgements**

This work was supported by Slovak Research and Development Agency through the project APVV-0069-15 and by the EU H2020-WIDESPREAD-05-2020 grant No. 952333, CasProt (Fostering high scientific quality in protein science in Eastern Slovakia).

## References

- [1] N.E. Chayen, Turning protein crystallisation from an art into a science, *Curr Opin Struct Biol.* 14 (2004) 577–583. <https://doi.org/10.1016/j.sbi.2004.08.002>.
- [2] C. di Guan, P. Li, P.D. Riggs, H. Inouye, Vectors that facilitate the expression and purification of foreign peptides in *Escherichia coli* by fusion to maltose-binding protein, *Gene.* 67 (1988) 21–30. [https://doi.org/10.1016/0378-1119\(88\)90004-2](https://doi.org/10.1016/0378-1119(88)90004-2).
- [3] C.V. Maina, P.D. Riggs, A.G. Grandea, B.E. Slatko, L.S. Moran, J.A. Tagliamonte, L.A. McReynolds, C.D. Guan, An *Escherichia coli* vector to express and purify foreign proteins by fusion to and separation from maltose-binding protein, *Gene.* 74 (1988) 365–373. [https://doi.org/10.1016/0378-1119\(88\)90170-9](https://doi.org/10.1016/0378-1119(88)90170-9).
- [4] D.B. Smith, K.S. Johnson, Single-step purification of polypeptides expressed in *Escherichia coli* as fusions with glutathione S-transferase, *Gene.* 67 (1988) 31–40. [https://doi.org/10.1016/0378-1119\(88\)90005-4](https://doi.org/10.1016/0378-1119(88)90005-4).
- [5] E.R. LaVallie, E.A. DiBlasio, S. Kovacic, K.L. Grant, P.F. Schendel, J.M. McCoy, A thioredoxin gene fusion expression system that circumvents inclusion body formation in the *E. coli* cytoplasm, *Biotechnology (N Y).* 11 (1993) 187–193. <https://doi.org/10.1038/nbt0293-187>.
- [6] D.S. Waugh, Making the most of affinity tags, *Trends Biotechnol.* 23 (2005) 316–320. <https://doi.org/10.1016/j.tibtech.2005.03.012>.
- [7] R.B. Kapust, D.S. Waugh, *Escherichia coli* maltose-binding protein is uncommonly effective at promoting the solubility of polypeptides to which it is fused., *Protein Sci.* 8 (1999) 1668–1674.
- [8] I. Kataeva, J. Chang, H. Xu, C.-H. Luan, J. Zhou, V.N. Uversky, D. Lin, P. Horanyi, Z.J. Liu, L.G. Ljungdahl, J. Rose, M. Luo, B.-C. Wang, Improving solubility of *Shewanella oneidensis* MR-1 and *Clostridium thermocellum* JW-20 proteins expressed into *Escherichia coli*, *J Proteome Res.* 4 (2005) 1942–1951. <https://doi.org/10.1021/pr050108j>.
- [9] R.-K. S, W. Ds, The ability to enhance the solubility of its fusion partners is an intrinsic property of maltose-binding protein but their folding is either spontaneous or chaperone-mediated., *PLoS One.* 7 (2012) e49589–e49589. <https://doi.org/10.1371/journal.pone.0049589>.
- [10] S. Raran-Kurussi, K. Keefe, D.S. Waugh, Positional effects of fusion partners on the yield and solubility of MBP fusion proteins, *Protein Expr Purif.* 110 (2015) 159–164. <https://doi.org/10.1016/j.pep.2015.03.004>.

- [11] E. Honjo, K. Watanabe, Expression of mature pokeweed antiviral protein with or without C-terminal extrapeptide in *Escherichia coli* as a fusion with maltose-binding protein, *Biosci Biotechnol Biochem.* 63 (1999) 1291–1294. <https://doi.org/10.1271/bbb.63.1291>.
- [12] D.P. Malinowski, M. Gourley, S. Edelstein, R.E. Pearson, Expression of a *Chlamydia* anticarbohydrate single-chain antibody as a maltose binding fusion protein, *Cell Biophys.* 21 (1992) 1–12. <https://doi.org/10.1007/BF02789473>.
- [13] F. Brégégère, J. Schwartz, H. Bedouelle, Bifunctional hybrids between the variable domains of an immunoglobulin and the maltose-binding protein of *Escherichia coli*: production, purification and antigen binding, *Protein Eng.* 7 (1994) 271–280.
- [14] A. Hayhurst, Improved expression characteristics of single-chain Fv fragments when fused downstream of the *Escherichia coli* maltose-binding protein or upstream of a single immunoglobulin-constant domain, *Protein Expr Purif.* 18 (2000) 1–10. <https://doi.org/10.1006/prev.1999.1164>.
- [15] V. Salema, L.Á. Fernández, High yield purification of nanobodies from the periplasm of *E. coli* as fusions with the maltose binding protein, *Protein Expr Purif.* 91 (2013) 42–48. <https://doi.org/10.1016/j.pep.2013.07.001>.
- [16] A. Korepanova, J.D. Moore, H.B. Nguyen, Y. Hua, T.A. Cross, F. Gao, Expression of membrane proteins from *Mycobacterium tuberculosis* in *Escherichia coli* as fusions with maltose binding protein, *Protein Expr Purif.* 53 (2007) 24–30. <https://doi.org/10.1016/j.pep.2006.11.022>.
- [17] A.A. Pioszak, H.E. Xu, Molecular recognition of parathyroid hormone by its G protein-coupled receptor, *Proc Natl Acad Sci U S A.* 105 (2008) 5034–5039. <https://doi.org/10.1073/pnas.0801027105>.
- [18] D.R. Smyth, M.K. Mrozkiewicz, W.J. McGrath, P. Listwan, B. Kobe, Crystal structures of fusion proteins with large-affinity tags, *Protein Sci.* 12 (2003) 1313–1322. <https://doi.org/10.1110/ps.0243403>.
- [19] Z.S. Derewenda, Application of protein engineering to enhance crystallizability and improve crystal properties, *Acta Crystallogr D Biol Crystallogr.* 66 (2010) 604–615. <https://doi.org/10.1107/S090744491000644X>.
- [20] D.S. Waugh, Crystal structures of MBP fusion proteins, *Protein Sci.* 25 (2016) 559–571. <https://doi.org/10.1002/pro.2863>.

- [21] T. Ferenci, U. Klotz, Affinity chromatographic isolation of the periplasmic maltose binding protein of *Escherichia coli*, *FEBS Letters*. 94 (1978) 213–217. [https://doi.org/10.1016/0014-5793\(78\)80940-5](https://doi.org/10.1016/0014-5793(78)80940-5).
- [22] S. Nallamsetty, B.P. Austin, K.J. Penrose, D.S. Waugh, Gateway vectors for the production of combinatorially-tagged His6-MBP fusion proteins in the cytoplasm and periplasm of *Escherichia coli*, *Protein Sci*. 14 (2005) 2964–2971. <https://doi.org/10.1110/ps.051718605>.
- [23] K.M. Routzahn, D.S. Waugh, Differential effects of supplementary affinity tags on the solubility of MBP fusion proteins, *J Struct Funct Genomics*. 2 (2002) 83–92. <https://doi.org/10.1023/a:1020424023207>.
- [24] P. Riggs, Expression and purification of recombinant proteins by fusion to maltose-binding protein, *Mol Biotechnol*. 15 (2000) 51–63. <https://doi.org/10.1385/MB:15:1:51>.
- [25] M.E. Kimple, A.L. Brill, R.L. Pasker, Overview of affinity tags for protein purification, *Curr Protoc Protein Sci*. 73 (2013) 9.9.1-9.9.23. <https://doi.org/10.1002/0471140864.ps0909s73>.
- [26] H.K. Binz, P. Amstutz, A. Kohl, M.T. Stumpp, C. Briand, P. Forrer, M.G. Grütter, A. Plückthun, High-affinity binders selected from designed ankyrin repeat protein libraries, *Nat Biotechnol*. 22 (2004) 575–582. <https://doi.org/10.1038/nbt962>.
- [27] S.K. Wetzel, G. Settanni, M. Kenig, H.K. Binz, A. Plückthun, Folding and unfolding mechanism of highly stable full-consensus ankyrin repeat proteins, *J Mol Biol*. 376 (2008) 241–257. <https://doi.org/10.1016/j.jmb.2007.11.046>.
- [28] J.F. Brandts, L.N. Lin, Study of strong to ultratight protein interactions using differential scanning calorimetry, *Biochemistry*. 29 (1990) 6927–6940. <https://doi.org/10.1021/bi00481a024>.
- [29] A.J. Sharff, L.E. Rodseth, J.C. Spurlino, F.A. Quiocho, Crystallographic evidence of a large ligand-induced hinge-twist motion between the two domains of the maltodextrin binding protein involved in active transport and chemotaxis, (n.d.) 7.
- [30] K. Döring, T. Surrey, P. Nollert, F. Jähnig, Effects of ligand binding on the internal dynamics of maltose-binding protein, *Eur J Biochem*. 266 (1999) 477–483. <https://doi.org/10.1046/j.1432-1327.1999.00880.x>.
- [31] J.S. Marvin, H.W. Hellenga, Manipulation of ligand binding affinity by exploitation of conformational coupling, *Nat Struct Biol*. 8 (2001) 795–798. <https://doi.org/10.1038/nsb0901-795>.

- [32] J. Hanes, A. Plückthun, In vitro selection and evolution of functional proteins by using ribosome display, *Proc Natl Acad Sci U S A.* 94 (1997) 4937–4942. <https://doi.org/10.1073/pnas.94.10.4937>.
- [33] D. Low, R. O’Leary, N.S. Pujar, Future of antibody purification, *J Chromatogr B Analyt Technol Biomed Life Sci.* 848 (2007) 48–63. <https://doi.org/10.1016/j.jchromb.2006.10.033>.
- [34] A.L. Cherry, C. Finta, M. Karlström, Q. Jin, T. Schwend, J. Astorga-Wells, R.A. Zubarev, M. Del Campo, A.R. Criswell, D. de Sanctis, L. Jovine, R. Toftgård, Structural basis of SUFU–GLI interaction in human Hedgehog signalling regulation, *Acta Crystallogr D Biol Crystallogr.* 69 (2013) 2563–2579. <https://doi.org/10.1107/S09074444913028473>.
- [35] S. Matsumoto, A. Shimada, D. Kohda, Crystal structure of the C-terminal globular domain of the third paralog of the *Archaeoglobus fulgidus* oligosaccharyltransferases, *BMC Structural Biology.* 13 (2013) 11. <https://doi.org/10.1186/1472-6807-13-11>.
- [36] D.M. Miller, J.S. Olson, J.W. Pflugrath, F.A. Quiocho, Rates of ligand binding to periplasmic proteins involved in bacterial transport and chemotaxis, *J Biol Chem.* 258 (1983) 13665–13672.

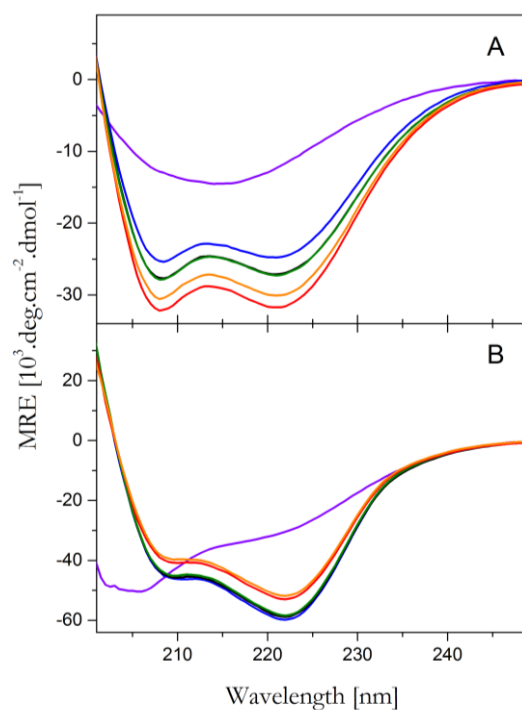
## Supporting information

to

### Efficient purification of MBP fusion proteins on DARPin affinity matrix

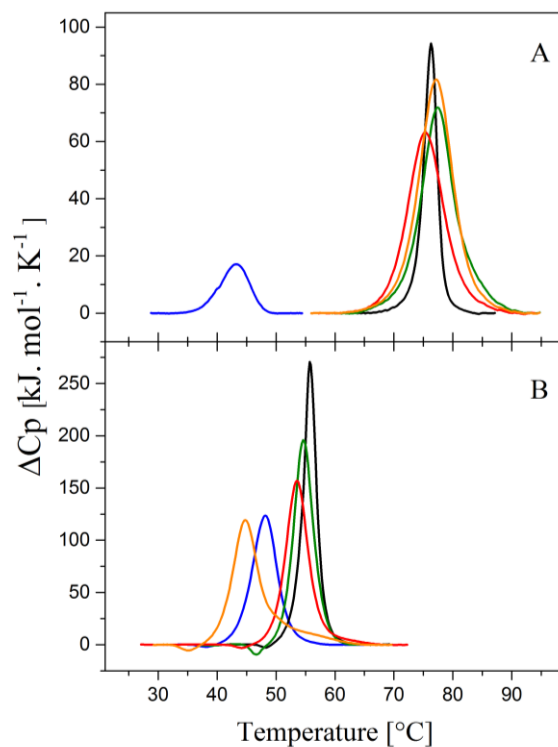
Michal Nemergut, Rostislav Škrabana, Andreas Plückthun, and Erik Sedlák

Figure S1



**Fig. S1.** CD spectra in the far-UV spectral region of DARPin off7 (A) and MBP (B) at pH 2.7 (purple), pH 3.5 (blue), pH 7.0 (black), pH 8.0 (green), pH 9.0 (red) and pH 10.0 (orange).

**Figure S2**



**Fig. S2.** DSC thermograms of DARPin off7 (A) and MBP (B) at pH 3.5 (**blue**), pH 7.0 (**black**), pH 8.0 (**green**), pH 9.0 (**red**) and pH 10.0 (**orange**).

**Figure S3**

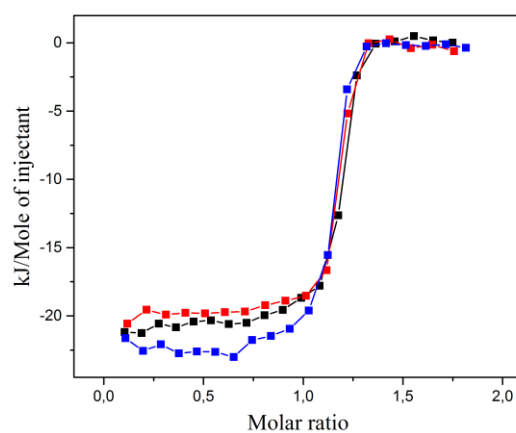


**Fig. S3.** The influence of maltose on the DARPin off7/MBP interaction. The ITC experiment was performed with maltose concentrations of 0 mM (**black**), 250 mM (**red**) and 400 mM (**blue**) in PBS pH 7.4.

**Figure S4**

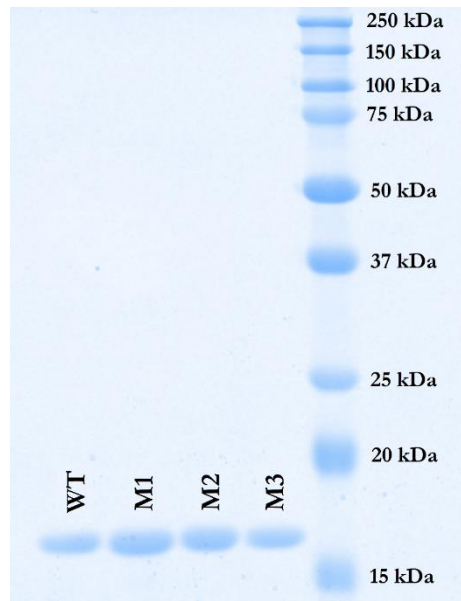


**Fig. S4.** A comparison of the purification of the DARPin mutants.

**Figure S5**

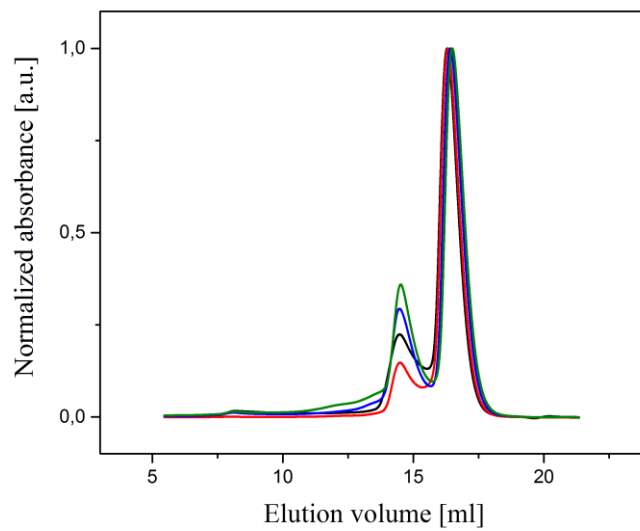


**Fig. S5.** Size exclusion chromatography of the DARPin mutants: wild type (**black**), M1 (**red**), M2 (**blue**) and M3 (**green**). Experiment was performed in phosphate-buffered saline at pH 7.4.



**Table S1.** Thermodynamic parameters of the interaction between DARPin off7 and MBP in the presence of different maltose concentration.

Parameters	0 M maltose	250 mM maltose	400 mM maltose
Stoichiometric ratio	1.0 ± 0.1	1.1 ± 0.1	1.1 ± 0.1
$K_D$ [nM]	47 ± 3.0	27 ± 1.0	40 ± 2.0
$\Delta H$ [kJ/mol]	-28.4 ± 0.2	-19.6 ± 0.2	-22.2 ± 0.1
$\Delta S$ [J/mol/K]	43.9 ± 1.2	78.2 ± 1.3	66.5 ± 1.4

**Table S2.** Thermodynamic parameters of the interaction between DARPin off7 mutants and MBP.

Parameters	WT-MBP	M1-MBP	M2-MBP	M3-MBP
Stoichiometric ratio	1.04 ± 0.1	1.09 ± 0.1	1.16 ± 0.1	1.12 ± 0.1
$K_D$ [nM]	47 ± 3.0	65 ± 4.0	114 ± 2.0	41 ± 2.0
$\Delta H$ [kJ/mol]	-28.4 ± 0.2	-24.4 ± 0.3	-16.7 ± 0.2	-20.1 ± 0.2
$\Delta S$ [J/mol/K]	43.9 ± 1.2	55.2 ± 2.5	76.7 ± 1.0	72.7 ± 0.8